3D source and receiver deghosting in the space-frequency domain using a depth-variable measurement surface: an initial off-shore synthetic data study with anticipated on-shore and ocean bottom application

Zhen Zhang and Arthur B. Weglein, M-OSRP/Physics Dept./University of Houston*

SUMMARY

Green's theorem derived deghosting methods in the space-frequency domain using a horizontal measurement surface (M.S.) have been successfully applied to synthetic and field data. Based on Green's theorem wavefield separation theory, this paper derives a 3D source and receiver deghosting formula for a depth-variable M.S. assuming its topography is known. In numerical tests, the model has a free surface and one horizontal reflector. We use the Cagniard-de Hoop method to generate synthetic data on horizontal, inclined, and undulated measurement surfaces, respectively. Numerical results show that the current Green's theorem deghosting formula for a constant depth M.S. remains useful for a mildly depth-variable M.S.. When the actual M.S. deviates significantly from horizontal, the horizontal M.S. formula produces serious errors and artifacts whereas the new formula produces an effective and satisfactory result. While the analysis and tests in this paper are based on nonhorizontal towed streamers, the motivation (and future work) is for on-shore and ocean bottom acquisition. Under these circumstances, the deviation from horizontal acquisition can be significant and the ability to accommodate a variable topography can have a considerably positive impact on subsequence processing and interpretation objectives.

INTRODUCTION

Deghosting is a long-standing seismic objective and problem (Amundsen (1993); Robinson and Treitel (2008)). It removes downgoing events of the recorded field (receiver ghost) and events first going up from source to air-water boundary (source ghost). Seismic resolution can be enhanced by removing spectrum notches and boosting low frequencies. Also, deghosting has risen in importance as prerequisites for free surface and internal multiple removal as well as for the resolution and delineation of imaged-inverted primaries (Weglein et al. (2002)).

The problem of accounting for the amplitude and phase distortions introduced by the so-called ghost effect was first studied in the context of sources by Van Melle and Weatherburn (1953). They showed that by using more than one source with a delayed firing pattern, it was possible to mitigate the ghost effect. Based on this, different acquisition techniques were proposed to achieve deghosting. These techniques include over/under streamers (Senneland et al. (1986); Posthumus (1993); Moldoveanu et al. (2007); Özdemir et al. (2008)), ocean bottom cable (OBC) (Barr et al. (1989)), hydrophone plus geophone (Carlson et al. (2007)) and multicomponent towed-streamers (Robertsson et al. (2008); Vassallo et al. (2013)). Other researchers started from signal characteristics of ghosts and designed specialized acquisition like single linearly slanted (Ray and Moore (1982); Dragoset and William (1991)) or depth-variable streamer (Soubaras et al. (2010)).

Motivated by progress in acquisition, different deghosting theories have developed. A more general and physically complete method of deghosting was provided using Green's theorem. Weglein et al. (2002) and Zhang et al. (2005, 2006) first developed that methodology and it was tested successfully by Zhang (2007). The first test on field data was reported by Mayhan and Weglein (2013). Tang (2014) analyzed the impact of acquisition on deghosting. For on-shore preprocessing, Wu and Weglein (2015a,b; 2016a,b) derived elastic Green's theorem wavefield separation methods in pressure and displacement space, and extended and applied it to on-shore and ocean bottom acquisition. Lin and Weglein (2016) studied the significance and impact of incorporating a 3D point source in Green's theorem deghosting. Zhang and Weglein (2016) studied 2D receiver deghosting in the space-frequency domain using a depth-variable tower streamer. The Green's theorem preprocessing methods are consistent with inverse scattering series (ISS) wave theory methods that do not require subsurface information (Weglein et al. (2003)). As pointed out by Weglein et al. (2003), every ISS isolated-task subseries requires (1) the removal of the reference wavefield, (2) estimation of the source signature and radiation pattern, and (3) source and receiver deghosting, and the ISS has a nonlinear dependence on these preprocessing steps. Green's theorem can offer a number of useful algorithms (see e.g. Zhang (2007); Mayhan (2013)) by choosing different reference medium to achieve different objectives (e.g. deghosting or P_0/P_s separation).

As pointed out by Mayhan and Weglein (2013) and Weglein et al. (2013), deghosting methods derived from the Green's theorem are wave-theoretic algorithms that can be defined in the frequency-space domain, and in principle can succeed with cables of any shape (e.g., slanted). The main purpose of including a nonhorizontal measurement surface (M.S.) is to accommodate on-shore and ocean bottom acquisition where deviation from horizontal acquisition can frequently occur. Therefore, based on Weglein et al. (2002), Zhang (2007) and Zhang and Weglein (2016), we derive a 3D source and receiver deghosting formula in the space-frequency domain for a depth-variable M.S., assuming the topography of M.S. is known. In numerical examples, we test the impact of assuming a horizontal M.S. (when M.S. is not actually horizontal) on deghosting and accommodation of a nonhorizontal M.S. using the new depth variable cable formula.

THEORY

Receiver side deghosting

Green's theorem derived seismic processing methods employ a model of the world that consists of a reference medium and sources (Weglein et al. (2003)). If we choose the reference medium to be a whole space of water (Figure 1b), whose property is the same as the actual medium (Figure 1a) along the measurement surface, the differences between the reference medium and the actual medium can be described as sources (Figure 1c) ρ, corresponding to the 'source' function or inhomogeneous driving force term(s) in a differential equation governing propagation in the reference medium. There are three sources required for the actual medium and experiment in Figure 1a, using a reference medium in Figure 1b. These three sources are the airgun ρ_{airgun}, the air perturbation ρ_{air}, and the earth perturbation ρ_{earth}, respectively, and $\rho = \rho_{air} + \rho_{airgun} + \rho_{earth}$.

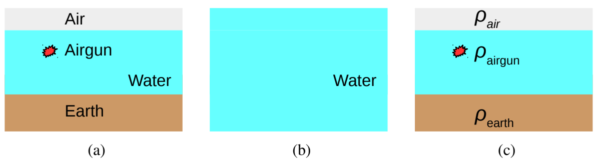

Figure 1: (a) Actual medium and experiment, (b) reference medium, and (c) three sources overlaid on the reference medium.

According to the Lippmann-Schwinger equation, the total wavefield at a location $\mathbf{r}$ can be expressed as,

$$P(\mathbf{r};\omega) = \int_{\infty} \rho(\mathbf{r}')G_0^+(\mathbf{r},\mathbf{r}';\omega)d\mathbf{r}' \tag{1}$$
$$= \int_{\infty} \rho_{air}G_0^+ d\mathbf{r}' + \int_{\infty} \rho_{airgun}G_0^+ d\mathbf{r}' + \int_{\infty} \rho_{earth}G_0^+ d\mathbf{r}'$$

Here $G_0^+(\mathbf{r},\mathbf{r}';\omega)$ is a causal Green's function for the homogeneous whole-space reference medium. Each of the three sources generates an outgoing wave (corresponding to the three terms of the right hand side of equation (1)), propagating straight away from the source point to the field point. Choose an enclosed volume V' that is bounded by surface S' (as shown by the dashed surface [- - -] in Figure 2) whose bottom surface is the measurement surface (M.S.) and whose top is an infinite hemisphere. It was shown by Weglein and Secrest (1990) that the Green's theorem derived surface integral,

$$\oint_{S'} \left[P(\mathbf{r}';\omega)\nabla_{\mathbf{r}'}G_0^+(\mathbf{r},\mathbf{r}';\omega) - G_0^+(\mathbf{r},\mathbf{r}';\omega)\nabla_{\mathbf{r}'}P(\mathbf{r}';\omega)\right]\cdot d\mathbf{S}' \tag{2}$$

represents the contribution to the wavefield at any location $\mathbf{r}$ inside the volume V', due to sources outside the volume V'. Here $d\mathbf{S}'$ is the surface element of S' at $\mathbf{r}'$ whose direction is outwards normal to S'. Since the chosen volume V' encloses the air and the airgun, the outside contribution only comes from ρ_{earth} beneath the M.S.. At any point $\mathbf{r} = \mathbf{r}_g$ within V', the integral in equation (2) gives the contribution of the total field due to the source outside ρ_{earth}. That contribution $\int \rho_{earth}G_0^+ d\mathbf{r}'$ is always propagating away from every point in ρ_{earth} and is always upgoing. If, in addition, the output point $\mathbf{r} = \mathbf{r}_g$ in equation (1) is chosen below ρ_{airgun} (and hence below ρ_{air}), then $\int_{V'}(\rho_{air} + \rho_{airgun})G_0^+ d\mathbf{r}'$ is downgoing at that point $\mathbf{r}$ inside V' and below ρ_{airgun}. For that type of output point, the $\int \rho_{earth}G_0^+ d\mathbf{r}'$ is both the contribution to the field in V' due to ρ_{earth} and the portion of field at $\mathbf{r}$ that is upgoing.

Therefore we can achieve receiver deghosting at $\mathbf{r}_g$ in terms of up/down separation (Weglein et al. (2002); Zhang et al. (2005)),

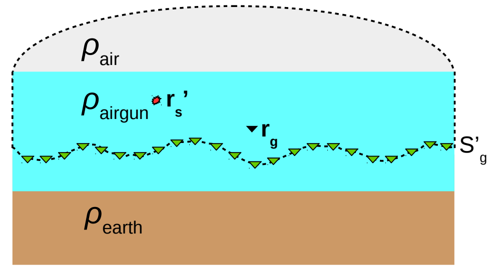

Figure 2: Configuration for receiver side deghosting.

$$P^{Rd}(\mathbf{r}_g;\omega) \tag{3}$$
$$= \oint_{S'} \left[P(\mathbf{r}';\omega)\nabla_{\mathbf{r}'}G_0^+(\mathbf{r}_g,\mathbf{r}';\omega) - G_0^+(\mathbf{r}_g,\mathbf{r}';\omega)\nabla_{\mathbf{r}'}P(\mathbf{r}';\omega)\right]\cdot d\mathbf{S}'$$

Here P^{Rd} means receiver deghosted data. We can prove that the integration over the hemisphere goes to zero as its radius goes to infinity, using Sommerfeld radiation condition. Hence,

$$P^{Rd}(\mathbf{r}_g;\omega) \tag{4}$$
$$= \int_{S'_g} \left[P(\mathbf{r}';\omega)\nabla_{\mathbf{r}'}G_0^+(\mathbf{r}_g,\mathbf{r}';\omega) - G_0^+(\mathbf{r}_g,\mathbf{r}';\omega)\nabla_{\mathbf{r}'}P(\mathbf{r}';\omega)\right]\cdot d\mathbf{S}'_g$$

Notice that both pressure and its normal derivative are needed. When the M.S. is horizontal, formula (4) reduces as below,

$$P^{Rd}(x_g,y_g,z_g;\omega) = \int_{S'_g} dx'_g dy'_g \tag{5}$$
$$\left\{P(x'_g,y'_g,z'_g;\omega)\frac{\partial}{\partial z''_g}G_0^+(x_g,y_g,z_g,x'_g,y'_g,z''_g;\omega)\Big|_{z''_g=z'_g} -\right.$$
$$\left. G_0^+(x_g,y_g,z_g,x'_g,y'_g,z'_g;\omega)\frac{\partial}{\partial z''_g}P(x'_g,y'_g,z''_g;\omega)\Big|_{z''_g=z'_g}\right\}$$

When the M.S. has some lateral variation in depth, meaning z'_g is a function of x'_g and y'_g, formula (4) reduces as below,

$$P^{Rd}(x_g,y_g,z_g;\omega) = \int_{S'_g} \left\{P(x'_g,y'_g,z'_g;\omega)\right. \tag{6}$$
$$\left(-\frac{1}{\Sigma}\frac{\partial z'_g}{\partial x'_g}\frac{\partial}{\partial x'_g} - \frac{1}{\Sigma}\frac{\partial z'_g}{\partial y'_g}\frac{\partial}{\partial y'_g} + \frac{1}{\Sigma}\frac{\partial}{\partial z'_g}\right)G_0^+(x_g,y_g,z_g,x'_g,y'_g,z'_g;\omega) -$$
$$\left. G_0^+(x_g,y_g,z_g,x'_g,y'_g,z'_g;\omega)\frac{\partial}{\partial n'}P(x'_g,y'_g,z'_g;\omega)\right\}\Sigma\, dx'_g dy'_g$$

where $\Sigma = \sqrt{1 + (\frac{\partial z'_g}{\partial x'_g})^2 + (\frac{\partial z'_g}{\partial y'_g})^2}$.

Source side deghosting

To further removes the source ghosts at $\mathbf{r}_g$, source deghosting is needed. Zhang (2007) and Mayhan (2013) explained the source deghosting in detail. Here we just introduce it briefly in three steps. The first step predicts the received data at $\mathbf{r}_g$ corresponding to energy sources at different $\mathbf{r}'_s$ on a horizontal surface S'_s, using Formula (4). This is shown by Figure 3a, where the black arrow (↗) represents the source ghosts that remains after receiver deghosting. The second step based on source-receiver reciprocity exchanges the locations of energy sources and receiver (as shown by Figure 3b). In this way, source ghosts up-going (↗) at the energy sources in Figure 3a are now receiver ghosts down-going (↙) at the "receivers". The third step predicts the "receiver" deghosted data (↖) at $\mathbf{r}_s = (x_s, y_s, z_s)$ (as shown by Figure 3b), with a second application of formula (5) as expressed by the formula below,

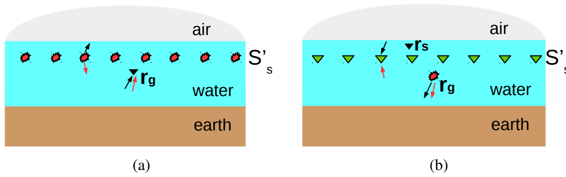

Figure 3: Principle of source side deghosting. (a) Firstly do receiver deghosting for multi sources, and then (b) after exchanging source and receiver, do "receiver" deghosting again.

$$
\begin{aligned}
&P^{SRd}(x_s, y_s, z_s, x_g, y_g, z_g; \omega) = \int_{S'_s} dx'_s\, dy'_s \qquad (7)\\
&\left\{ P^{rd}(x_g, y_g, z_g, x'_s, y'_s, z'_s; \omega) \frac{\partial}{\partial z''_s} G_0^+(x_s, y_s, z_s, x'_s, y'_s, z''_s; \omega)\Big|_{z''_s = z'_s} - \right.\\
&\left. G_0^+(x_s, y_s, z_s, x'_s, y'_s, z'_s; \omega) \frac{\partial}{\partial z''_s} P^{rd}(x_g, y_g, z_g, x'_s, y'_s, z''_s; \omega)\Big|_{z''_s = z'_s} \right\}
\end{aligned}
$$

P^{SRd} represents the deghosted data that has no source or receiver ghosts. Since this wave goes downward from $\mathbf{r}_g$ and gets upward to $\mathbf{r}_s$, $P^{SRd}(x_g, y_g, z_g, x_s, y_s, z_s; \omega)$ is equal to $P^{SRd}(x_s, y_s, z_s, x_g, y_g, z_g; \omega)$ based on reciprocity. Therefore, formula (4) and formula (7) together predict the source and receiver deghosted data at $\mathbf{r}_g$. In numerical examples below, we will compare deghosting results using formula (5) and formula (7) with results using formula (6) and formula (7).

NUMERICAL EXAMPLES

Velocity model is shown in Figure 4. It has a free surface and a horizontal reflector at the depth of 50m. Below there are three numerical examples that generate total wave on respectively
(1) horizontal M.S. and then do deghosting (using formula (5) and formula (7)),
(2) inclined M.S. and then do deghosting, with assuming that the M.S. is horizontal in deghosting (using formula (5) and formula (7)), and
(3) undulated M.S. and then do deghosting, with firstly assuming that the M.S. is horizontal in deghosting (using formula (5) and formula (7)) and with accommodation of the topography of M.S. in deghosting (using formula (6) and formula (7)).

Flat measurement surface

Figure 5a shows the total wave generated at constant depth 35m. We can see the primary, free surface mutiple and ghosts interfere with each other, especially at far offset. Figure 6a shows the deghosted data predicted at 15m depth using formula (5) and formula (7). We can see clearly two events of opposite polarity which are the primary and free surface multiple, respectively.

Inclined measurement surface

Figure 6b shows the deghosted data predicted at 15m depth, using data generated on 2° M.S. but assuming it's horizontal M.S. in deghosting (using formula (5) and formula (7)). We can hardly see any difference between Figure 6a and Figure 6b.

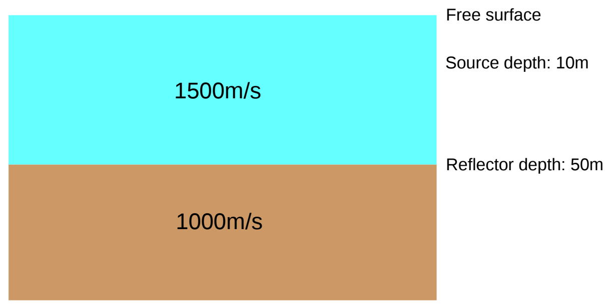

Figure 4: Velocity model and source position. The source is at 10m depth. The horizontal reflector is at 50m depth.

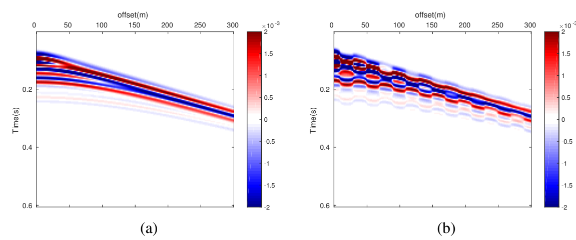

Figure 5: Data generated by the Cagniard-de Hoop method. **(a)** Horizontal M.S. at depth of 35m, and **(b)** undulated M.S. with minimum depth of 25m and maximum depth of 45m

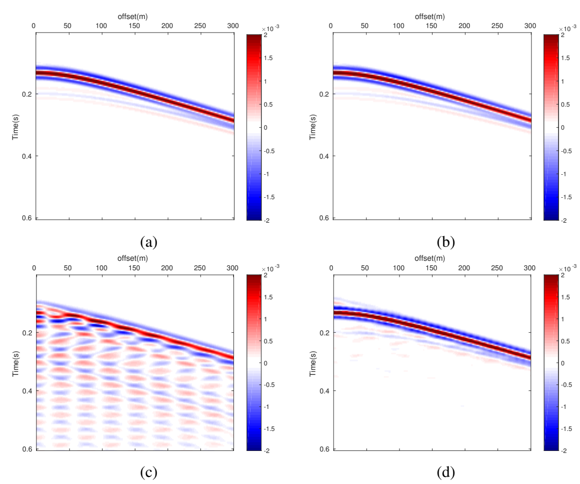

Figure 6: Section of deghosting data predicted at 15m depth. **(a)** M.S. is actually horizontal, **(b)** M.S. is 2° inclined, assuming it's horizontal in deghosting, **(c)** M.S. is undulated, assuming it's horizontal in deghosting, and **(d)** M.S. is undulated, with accommodation in deghosting

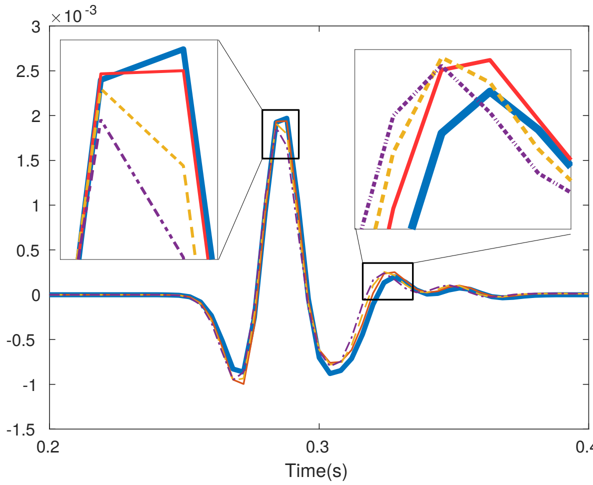

(a)

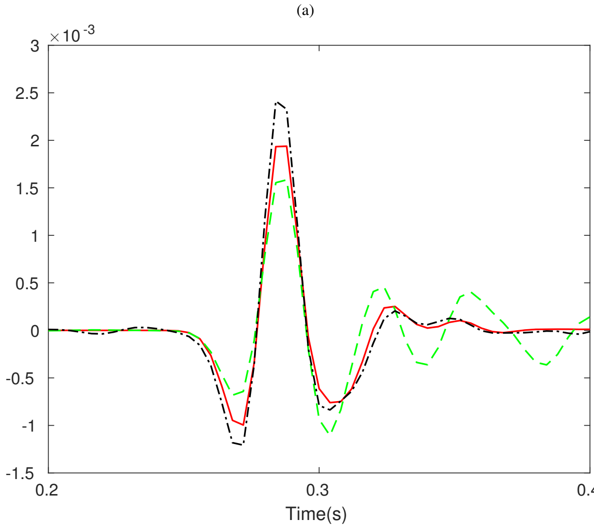

(b)

Figure 7: Traceplot of deghosting data predicted at 15m depth. **(a)** Traceplot (offset=300m) comparison of actual primary and free surface multiple (generated by the Cagniard-de Hoop method) at 15m depth (▬), deghosted result (Figure 6a) using total wave generated on horizontal M.S. (—), deghosted result using total wave generated on 1° inclined M.S. assuming it's horizontal in deghosting (- - -) and deghosted result (Figure 6b) using total wave generated on 2° inclined M.S. assuming it's horizontal in deghosting (- · · · - -), and
(b) traceplot (offset=300m) comparison of deghosted result (Figure 6a) using total wave generated on horizontal M.S. (—), deghosted result (Figure 6c) using total wave generated on undulated M.S. assuming it's horizontal in deghosting (- - -) and deghosted result (Figure 6d) using total wave generated on undulated M.S. with accommodation of the M.S.'s topography in deghosting (- · - · -)

To see clearly the effectiveness of Figure 6a and Figure 6b so that we know the impact of the inclination of M.S., Figure 7a show the comparison in one trace between perfect deghosted data generated by the Cagniard-de Hoop method (which is primary and free surface multiple) and actual deghosted results that assumes horizontal M.S. in deghosting. We can see the deghosting result (—) using actually horizontal M.S. is very close to perfect. This means the deghosting method itself for actually horizontal M.S. (formula (5) and formula (7)) is very effective. Also we can see the result using 1° inclined M.S. (- - -) deviates only a little from it (—) and the result using 2° inclined M.S. (- · · · - -) just deviates a little more. This means that although the assumption of horizontal M.S. in deghosting can bring deviation from perfect deghosted data, such deviation is very slight when the M.S. is close to horizontal.

Undulating measurement surface

Figure 5b shows the total wave generated on periodically undulated M.S. with miminum depth 25m and maximum depth 45m. And undulation period is 40m. Figure 6c shows the deghosted data predicted at 15m depth, assuming horizontal M.S. in deghosting (using formula (5) and (7)). We can see many periodical artifacts. Figure 6d shows the deghosting result that accommodates the topography of M.S. in deghosting (using formula (6) and (7)). Almost all artifacts disappear and the result is close to Figure 6a.

Figure 7b compares the trace (offset=300m) of Figure 6a, Figure 6c and Figure 6d. We can see the result (- - -) using formula (5) and (7) fails when the M.S. has obvious undulation. In contrast, with accommodation of the topography of undulated M.S., the result (- · - · -) using formula (6) and (7) retains the effectiveness of result (—) of which the M.S. is originally horizontal.

CONCLUSIONS

The Green's theorem source and receiver deghosting algorithm is developed and tested for depth-variable towed streamers. This is relevant for ocean bottom preprocessing when the ocean bottom is nonflat, and for on-shore preprocessing since the earth's surface can have significant lateral variability. Numerical examples show that if data are acquired on a non-horizontal measurement surface (M.S.), the constant depth assumption can provide effective deghosting results when the M.S. is close to horizontal. If the M.S. deviates significantly from horizontal, the conventional deghosting method that assumes a horizontal M.S. may lead to an inaccurate result. In the latter case, the Green's theorem deghosting formula proposed in this paper can provide effective deghosting results, by incorporating the topography of the M.S.. This is important for subsequent processing including multiple removal. This step, the Green's theorem deghosting for towed streamer data, can be extended and utilized for on-shore and ocean bottom acquisition, where the M.S. can at times be far from horizontal.

ACKNOWLEDGEMENTS

We thank the M-OSRP sponsors for their encouragement and support. We would like to thank Dr. Jingfeng Zhang of BP for his fundamental work. We would like to thank Dr. Jim Mayhan for his suggestion in the language writing of this paper.

EDITED REFERENCES

Note: This reference list is a copyedited version of the reference list submitted by the author. Reference lists for the 2017 SEG Technical Program Expanded Abstracts have been copyedited so that references provided with the online metadata for each paper will achieve a high degree of linking to cited sources that appear on the Web.

REFERENCES

Amundsen, L., 1993, Wavenumber-based filtering of marine point-source data: Geophysics, **58**, 1335–1348, http://doi.org/10.1190/1.1443516.

Barr, F. J., and J. I. Sanders, 1989, Attenuation of water-column reverberations using pressure and velocity detectors in a water-bottom cable: 59th Annual International Meeting, SEG, Expanded Abstracts, 653–656, http://doi.org/10.1190/1.1889557.

Carlson, D., A. Long, W. Söllner, H. Tabti, R. Tenghamn, and N. Lunde, 2007, Increased resolution and penetration from a towed dual-sensor streamer: First Break, **25**, 71–77.

Dragoset Jr, William H., 1991, Processing for seismic data from slanted cable: U. S. Patent 4,992,992.

Lin, X., and A. B. Weglein, 2016, The significance and impact of incorporating a 3d point source in green's theorem deghosting: 86th Annual International Meeting, SEG, Expanded Abstracts, 4766–4771, http://doi.org/10.1190/segam2016-13955971.1.

Mayhan, J., 2013, Wave-theoretic preprocessing to allow the inverse scattering series methods for multiple removal and depth imaging to realize their potential and impact: Ph.D. dissertation, University of Houston.

Mayhan, J. D., and A. B. Weglein, 2013, First application of Green's theorem-derived source and receiver deghosting on deep-water gulf of mexico synthetic (seam) and field data: Geophysics, **78**, WA77–WA89, http://doi.org/10.1190/GEO2012-0295.1.

Moldoveanu, N., L. Combee, M. Egan, G. Hampson, L. Sydora, and W. Abriel, 2007, Seismic-over/under towed-streamer acquisition: A method to extend seismic bandwidth to both higher and lower frequencies: The Leading Edge, **26**, 41–58, http://doi.org/10.1190/1.2431831.

Özdemir, A. K., P. Caprioli, A. Özbek, E. Kragh, and J. O. Robertsson, 2008, Optimized deghosting of over/under towed-streamer data in the presence of noise: The Leading Edge, **27**, 190–199, http://doi.org/10.1190/1.2840366.

Posthumus, B., 1993, Deghosting using a twin streamer configuration: Geophysical Prospecting, **41**, 267–286, http://doi.org/10.1111/j.1365-2478.1993.tb00570.x.

Ray, C. H., and N. A. Moore, 1982, High resolution, marine seismic stratigraphic system: U.S. Patent 4,353,121.

Robertsson, J. O., I. Moore, M. Vassallo, K. Özdemir, D. J. van Manen, and A. Özbek, 2008, On the use of multicomponent streamer recordings for reconstruction of pressure wavefields in the crossline direction: Geophysics, **73**, no. 5, A45–A49, http://doi.org/10.1190/1.2953338.

Robinson, E. A., and S. Treitel, 2008, Digital imaging and deconvolution: The abcs of seismic exploration and processing: Society of Exploration Geophysicists, https://doi.org/10.1190/1.9781560801610.

Senneland, L., L. Berg, A. Haugen, B. Fotland, and J. Vestby, 1986, 2-D deghosting using vertical receiver arrays: 56th Annual International Meeting, SEG, Expanded Abstracts, 516–519, http://doi.org/10.1190/1.1893019.

Soubaras, R., 2010, Deghosting by joint deconvolution of a migration and a mirror migration: 80th Annual International Meeting, SEG, Expanded Abstracts, 3406–3410, https://doi.org/10.1190/1.3513556.

Tang, L., 2014, Developing and analyzing Green's theorem methods to satisfy prerequisites of inverse scattering series multiple attenuation for different types of marine acquisition and extending prerequisite satisfaction to on-shore exploration: Ph. D. dissertation, University of Houston.

Van Melle, F., and K. Weatherburn, 1953, Ghost reflections caused by energy initially reflected above the level of the shot: Geophysics, **18**, 793–804, http://doi.org/10.1190/1.1437929.
Vassallo, M., K. Eggenberger, D.-J. van Manen, A. Özbek, and P. Watterson, 2013, Broadband and beyond with marine towed streamers: The Leading Edge, **32**, 1356–1365.
Weglein, A. B., and B. G. Secrest, 1990, Wavelet estimation for a multidimensional acoustic or elastic earth: Geophysics, **55**, 902–913, http://doi.org/10.1190/1.1442905.
Weglein, A. B., S. Shaw, K. Matson, J. Sheiman, R. Stolt, T. Tan, A. Osen, G. Correa, K. Innanen, Z. Guo, and J. Zhang, 2002, New approaches to deghosting towed-streamer and ocean-bottom pressure measurements: 72th Annual International Meeting, SEG, Expanded Abstracts, 2114–2117, http://doi.org/10.1190/1.1817121.
Weglein, A. B., F. V. Araújo, P. M. Carvalho, R. H. Stolt, K. H. Matson, R. T. Coates, D. Corrigan, D. J. Foster, S. A. Shaw, and H. Zhang, 2003, Inverse scattering series and seismic exploration: Inverse problems, **19**, R27–R83, http://doi.org/10.1088/0266-5611/19/6/R01.
Weglein, A. B., J. D. Mayhan, L. Amundsen, H. Liang, J. Wu, L. Tang, Y. Luo, and Q. Fu, 2013, Green's theorem deghosting algorithms in (k, omega)(eg, p-vz deghosting) as a special case of (x, omega) algorithms (based on Green's theorem): Journal of Seismic Exploration, **22**, 389–412.
Wu, J., and A. B. Weglein, 2015a, Preprocessing in displacement space for on-shore seismic processing: Removing ground roll and ghosts without damaging the reflection data: 85th Annual International Meeting, SEG, Expanded Abstracts, 4626–4630, http://doi.org/10.1190/segam2015-5879845.1.
Wu, J., and A. B. Weglein, 2015b, Preprocessing in the ps space for on-shore seismic processing: Removing ground roll and ghosts without damaging the reflection data: 85th Annual International Meeting, SEG, Expanded Abstracts, 4740–4744, http://doi.org/10.1190/segam2015-5907507.1.
Wu, J., and A. B. Weglein, 2016a, Green's theorem-based onshore preprocessing: A reduced data requirement assuming a vacuum/earth model for the air/earth interface and the evaluation of the usefulness of that assumption: 86th Annual International Meeting, SEG, Expanded Abstracts, 4685–4689, http://doi.org/10.1190/segam2016-13956378.1.
Wu, J., and A. B. Weglein, 2016b, Predicting deghosted reflection data for both pressure and multicomponent displacements at the ocean bottom: 86th Annual International Meeting, SEG, Expanded Abstracts, 4751–4755, http://doi.org/10.1190/segam2016-13868798.1.
Zhang, J., 2007, Wave theory based data preparation for inverse scattering multiple removal, depth imaging and parameter estimation: Ph. D. dissertation, University of Houston.
Zhang, J. and A. B. Weglein, 2005, Extinction theorem deghosting method using towed streamer pressure data: 75th Annual International Meeting, SEG, Expanded Abstracts, 2095–2098, http://doi.org/10.1190/1.2148125.
Zhang, J. and A. B. Weglein, 2006, Application of extinction theorem deghosting method on ocean bottom data: 76th Annual International Meeting, SEG, Expanded Abstracts, 2674–2678, http://doi.org/10.1190/1.2370077.
Zhang, Z., and A. B. Weglein, 2016, 2D Green's theorem receiver deghosting in the (x-omega) domain using a depth-variable cable towards on-shore and ocean-bottom application with variable topography: 86th Annual International Meeting, SEG, Expanded Abstracts, 4735–4740, http://doi.org/10.1190/segam2016-13956004.1.